HNPS Advances in Nuclear Physics

Vol 30 (2024)

HNPS2023

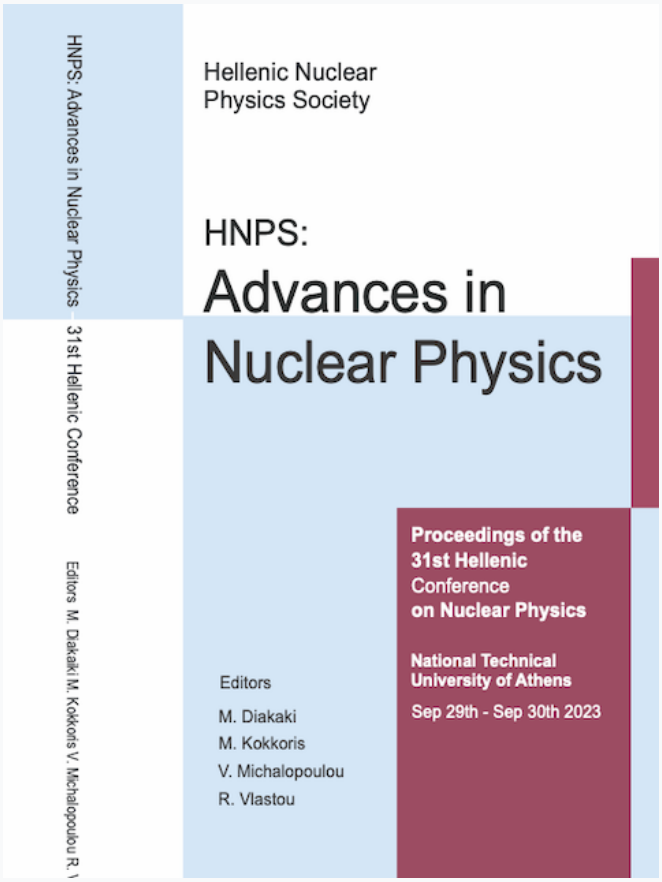

The ELISA spectrometer at the JRC-Geel: development, achievements and future plans

Georgios Gkatis, Elisa Pirovano, Maria Diakaki, Gilles Noguere, Markus Nyman, Andreea Oprea, Carlos Paradela, Arjan Plompen

doi: 10.12681/hnpsanp.6288

To cite this article:

Gkatis, G., Pirovano, E., Diakaki, M., Noguere, G., Nyman, M., Oprea, A., Paradela, C., & Plompen, A. (2024). The ELISA spectrometer at the JRC-Geel: development, achievements and future plans. *HNPS Advances in Nuclear Physics*, *30*, 11–18. https://doi.org/10.12681/hnpsanp.6288

The ELISA spectrometer at the JRC-Geel: development, achievements and future plans

G. Gkatis[1,2,*], E. Pirovano[3], M. Diakaki[2], G. Noguere[1], M. Nyman[4], A. Oprea[5], C. Paradela[5], and A.J.M. Plompen[5]

[1] *CEA/DES/IRESNE/DER/SPRC/LEPh, Cadarache, F-13108 Saint Paul Lez Durance, France*
[2] *Department of Physics, National Technical University of Athens, GR-15780 Athens, Greece*
[3] *Physikalisch-Technische Bundesanstalt, D-38116 Braunschweig, Germany*
[4] *Department of Chemistry, University of Helsinki, FI-00014 Helsinki, Finland*
[5] *European Commission, Joint Research Centre, B-2440 Geel, Belgium*

Abstract The ELISA (ELastic and Inelastic Scattering Array) setup, currently installed at the GELINA (Geel Electron Linear Accelerator) facility of the EC-JRC (European Commission – Joint Research Centre) in Geel (Belgium), is a unique instrument in Europe, used for the production of high-resolution neutron elastic and inelastic scattering cross-section data, relevant for nuclear physics applications. The setup features 32 liquid organic scintillators for the detection of the scattered neutrons coupled with a ^{235}U ionization chamber for the measurement of the neutron flux. This contribution outlines a brief history of the development of the setup, the measurements that have been performed so far, and the future experimental plans.

Keywords neutron spectrometry, elastic scattering, cross-section, angular distributions

INTRODUCTION

Neutron elastic scattering cross section data are very important in nuclear physics, playing a pivotal role in understanding the complex interactions between neutrons and atomic nuclei. These data are used in a plethora of physics applications, from nuclear reactor technology to nuclear astrophysics, medicine, material science, and many more, shaping our understanding of fundamental processes and enabling innovations in diverse fields. In the case of nuclear power reactors, these data are indispensable for the design and optimization of reactors, ensuring safe operation and enhancing overall efficiency. Angular distributions of neutron elastic scattering are necessary to study the spatial distribution and energy spectrum of neutrons within a reactor core, providing key information for the control and manipulation of the neutron flux, which, in turn, affects the rate of nuclear reactions and overall power generation. In practice, elastic scattering represents the dominant scattering mechanism, a reaction channel that is always open, especially in the fast neutron region, where in most cases, it amounts to almost 50% of the total cross section.

Additionally, high energy-resolution neutron elastic scattering cross section data are playing a crucial role in theoretical studies of nuclear reactions, providing critical input for developing and refining models that describe the interaction between neutrons and atomic nuclei. For example, the nuclear optical potential model heavily relies on accurate cross section data of proton and neutron elastic scattering in order to correctly determine the potential parameters [1-3]. These models are essential for interpreting experimental results, predicting nuclear reaction cross sections under diverse conditions, and advancing our comprehension of nuclear structure.

The experimental determination of neutron elastic scattering cross sections poses a challenge due to several factors. Firstly, since neutrons lack electric charge, direct detection is almost impossible. In most cases, neutrons are detected indirectly based on the measurement of secondary particles produced

* Corresponding author: *georgios.gkatis@cea.fr*

by neutron interactions using scintillation detectors, proportional counters, or solid-state detectors. Furthermore, the angular dependence of neutron scattering has to be taken into account, which creates a need to measure multiple detection angles. Additionally, the scattering samples must be of high purity in order to avoid extra corrections and uncertainties. Finally, background interference plays a crucial role in the extraction of meaningful data. Neutron scattering experiments need to be conducted in environments with low background radiation, ideally in a vacuum, to avoid signals generated from in-beam neutrons scattering on air and then reaching the detectors. Given these challenges, experimentalists need to employ meticulous techniques and sophisticated data analysis methods to properly measure elastic scattering cross sections.

In this context, the present contribution is dedicated to the description of the ELISA spectrometer [4-7] operating at the GELINA facility of the EC-JRC in Geel, Belgium, used for high resolution neutron scattering cross section data measurements in the fast neutron energy region. This setup uses neutron spectrometry coupled with the time-of-flight technique to determine the neutron incident and detection energy, respectively. A short description of the GELINA facility, the development of the ELISA setup, and the data analysis procedure is given. The future plans for the setup are also discussed in the end.

THE ELISA SPECTROMETER

ELISA (ELastic and Inelastic Scattering Array) is one of the various experimental setups installed at the GELINA neutron time-of-flight facility [8] of the EC-JRC in Geel. GELINA is a pulsed white neutron source, currently operating at 800 Hz repetition rate, with a typical time resolution of 2 ns. Accelerated electrons are impinging on a depleted uranium target, producing strong bremsstrahlung radiation. The neutrons are generated via the photo-nuclear reactions ^{238}U(γ,n) – ^{238}U(γ,f). They are emitted isotropically, and travel through the various flight paths (8 to 400 m), distributed at different angles, up to the measurement cabins where the sample under study and the detection setup are installed.

The concept of measuring double differential neutron-emission cross sections dates back to the end of the eighties, when a similar detector array, featuring 8 liquid organic scintillators, was designed and developed at GELINA [8]. The development of ELISA was based on this past experience. One of the main differences between the two setups is that in the old array, the detectors were placed as close as possible to the sample without interfering with the neutron beam, while at ELISA, the detection angles were carefully chosen based on the possibility of applying numerical techniques for the angle integration. To achieve high accuracy in the detection angles, the distance between the detectors and the sample position had to be increased.

The development of the ELISA spectrometer was initiated in 2013 and finished in 2016. Photos of the setup development phase are given in Fig. 1, in chronological order. The first version of the supporting frame was constructed and placed in the 100 m station of flight path 3 (FP3_100m). The first 8 detectors were tested and characterized using γ-ray sources. Then, in 2015, the final version of the frame was constructed and placed in the 30 m station of flight path 1 (FP1_30m), where it was properly aligned. The setup, in its final form, consists of 32 liquid organic scintillators for the detection of the scattered neutrons, coupled to a ^{235}U ionization chamber for the measurement of the neutron flux. The scintillators are divided into 4 sets of 8 detectors, each mounted at specific angles with respect to the neutron beam direction (Table 1).

All 32 detectors are liquid organic scintillators, commercially available from Scionix. They have a cylindrical shape with a liquid volume cell of 2.54 cm radius and 5.08 cm height. The cells are filled up to 97% with the scintillation liquid, leaving a 3% expansion void bubble. They have an aluminum housing of 1.52 mm thickness, sealed with a quartz window that provides an optical coupling to the photomultiplier tube (PMT, Electron Tubes Ltd., model 9213). In Fig. 2, an X-ray scan of one of the

detectors is presented in (a), where the void in the liquid volume cell and the electronic circuits of the PMT are visible, and in (b), a detailed description of the geometry of the detectors, as used in the model, is given. Half of them are filled with the EJ315 scintillation material (by Eljen Technology), using highly purified deuterated benzene (C_6D_6) (model: 51A51/2MQOE1-EJ315-NX) [9], and the other half are filled with the EJ301 material, a liquid based on xylene (C_8H_{10}) (model: 51A51/2MQOE1-EJ301-NX) [10]. Both detectors types have a time resolution of less than 1 ns, making them suitable for time-of-flight measurements. The reason behind choosing two different types of scintillation material lies in the fact that the two different response functions, produced for the proton-based (EJ301) and deuterium-based (EJ315), respectively, allow for the discovery of errors during the analysis procedure and act as a cross-check between the extracted results. In Table 2 the composition and physical properties of the two materials are given.

Table 1. *The 8 different detection angles with respect to the neutron beam direction. Their corresponding cosine and weights used for the numerical quadrature are also given.*

Angle (deg)	163.8	142.8	121.7	100.6	79.4	58.3	36.2	16.2
Cosine	-0.9603	-0.7967	-0.5255	-0.1834	0.1834	0.5255	0.7967	0.9603
Weight	0.1012	0.2224	0.3137	0.3627	0.3627	0.3137	0.2224	0.1012

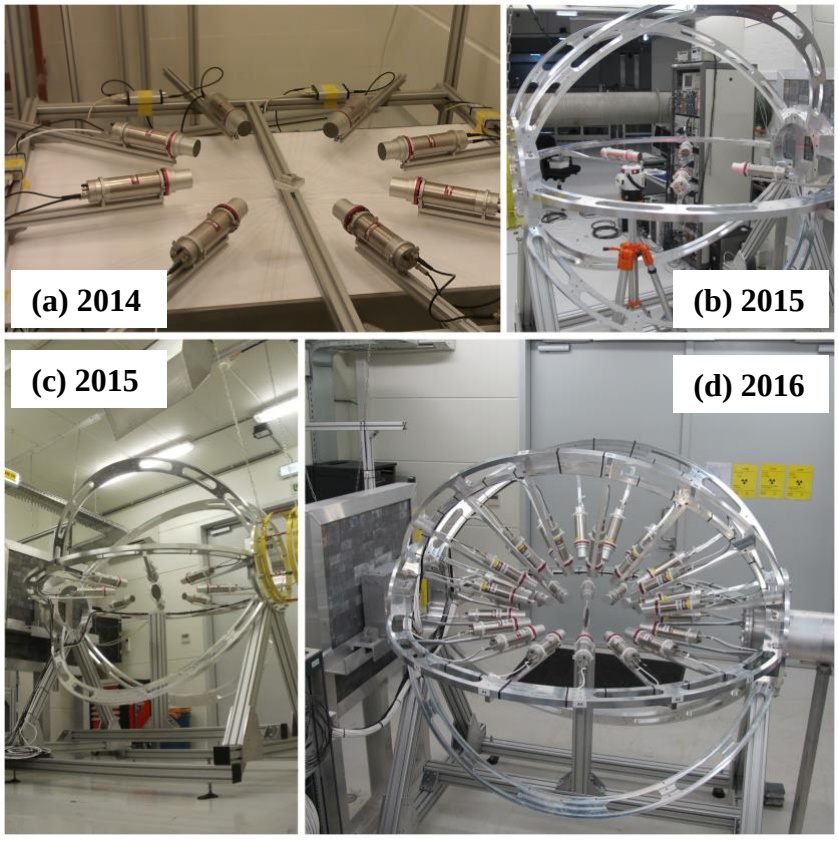

Figure 1. *Chronological development of the ELISA setup. (a) 2014: The initial frame of the setup, with the first 8 detectors placed at the 100 m station of flight path 3. (b) 2015: The alignment of the newly constructed supporting frame. (c) 2015: The new aligned frame with the first 8 detectors is now placed at the 30 m station of flight path 1. (d) 2016: The final state of the setup with all 32 detectors.*

For the data acquisition of the scintillators, a dedicated digitizer-based system was developed at GELINA. It features 8 digitizer cards with 4 channels each, manufactured by SP Devices (model:

ADQ14DC-4A-VG-PXIe). The cards have a 500 MS/s sampling rate and 14 bit resolution. They are installed in a PXIe chassis (ADLINK PXES-2780) and controlled via a Red Hat Enterprise Linux 6.4 operating system. The digitizer's clocks are synchronized by an external 10 MHz reference coming from a clock generator (Stanford Research Systems Inc. CG635). The signals are recorded from the anode output of the PMT of each detector. Every channel triggers independently of the other when a signal surpasses the given threshold. The timestamps of the recorded signals are directly relative to the linac reference signal ("T0 signal"), which is connected to the digitizers as an external signal and resets the time for every neutron burst. All recorded signal information, including waveforms and timestamps, are saved on the disk for offline analysis.

Table 2. *Composition and physical properties of the EJ301 and EJ315 scintillation materials [9-10]*

	EJ301	**EJ315**
Number of ^{1}H atoms per cm^2	4.82×10^{22}	0.0287×10^{22}
Number of ^{2}H atoms per cm^2	-	4.06×10^{22}
Number of C atoms per cm^2	3.98×10^{22}	4.10×10^{22}
Density at 25°C (g/cm^3)	0.874	0.954
Scintillation liquid volume (cm^3)	105.9	105.9
Scintillation efficiency (photons/1 MeV electrons)	12000	9200
Wavelength of maximum emission (nm)	425	425

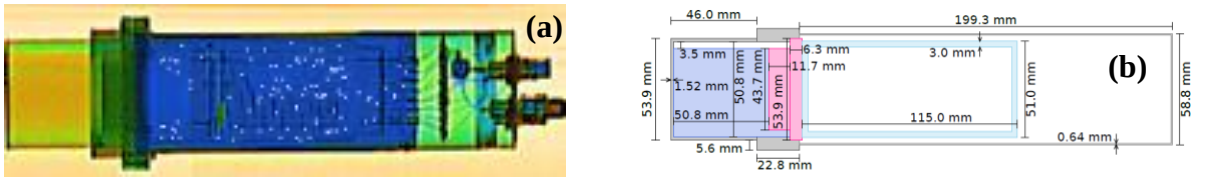

Figure 2. *a) X-ray scan of one of the detectors used at the ELISA setup. The liquid volume cell, the void in it, and the electronic circuits of the PMT are visible. b) Description of the geometry of the detectors is presented [4].*

All cross sections measured with the ELISA setup are relative to the standard ^{235}U neutron induced fission cross section. For that, a ^{235}U ionization chamber is placed upstream, 1.37 m from the sample position (behind the lead wall in Fig. 1 (d)). The chamber contains 8 UF_4 deposits on top of two single sided and three double sided aluminum foils. The foils are 84 mm in diameter and 20 μm in thickness. The samples were manufactured at the EC-JRC Geel, using the vacuum evaporation technique and have a diameter of 70 mm, based on the diameter of the evaporation mask that was used. In Table 3, the uranium content of each sample and the isotopic composition of the material that was used are reported. The deposits are placed into the chamber at a distance of 14 mm from each other, with the single sided foils staying at the two ends of the chamber. For the detection of the fission fragments, aluminum electrodes of 25 μm thickness serves as cathodes, at 7 mm distance from the deposits. In Fig. 3, the stack of the deposits and the electrodes inside the chamber are presented. A steady flow of P10 gas (10% methane, 90% argon) at atmospheric pressure is provided into the chamber.

The data acquisition system of the chamber consists of conventional NIM electronics. In the beginning, the recorded signal is fed to a charge integration preamplifier (CSTA2HV from the Technische Universitat Darmstadt), and then it is split into two directions. On one side, the signal goes through a fast filter amplifier (Ortec 579), then to a constant fraction discriminator (CFD, Ortec 584), and ends up to a time to digital converter (TDC, JRC in-house developed). On the other side, the signal passes through a spectroscopic amplifier (Ortec 671) and then to an analog to digital converter (ADC, FAST ComTec 7072). In the end, the signals coming from the TDC and the ADC are fed to a

multiplexer (MMPM, JRC in-house developed), which makes sure the recorded amplitude and time information are synchronized, and saved for offline analysis.

Table 3. *Areal density of the UF_4 deposits. The uranium content was determined by alpha counting, the UF_4 content was calculated from the 1:4 molar ratio, and the ^{235}U amount was calculated based on the isotopic composition report at the bottom of the table.*

Target	**μg U/cm^2**	**μg UF_4/cm^2**	**μg ^{235}U/cm^2**
Target 1	622(1)	823(2)	622(1)
Target 2 side 1	488(1)	646(2)	488(1)
Target 2 side 2	464(1)	614(1)	463(1)
Target 3 side 1	489(1)	647(2)	488(1)
Target 3 side 2	459(1)	607(2)	458(1)
Target 4 side 1	487(1)	645(2)	487(1)
Target 4 side2	461(1)	610(2)	461(1)
Target 5	628(1)	831(2)	628(1)

U-isotope	^{233}U	^{234}U	^{235}U	^{236}U	^{238}U
Abundance	< 0.001	0.036	99.94	0.011	0.013

DATA ANALYSIS PROCEDURE

The analysis of the scintillator data is a multi-step, complex process described in detail in Ref. [4]. Here, only a short overview of the analysis is given. The steps of the data analysis are the following:

- Offline processing of the recorded waveforms.
- Subtraction of the background contribution.
- Complete characterization of the neutron response functions of the detectors.
- Separation between elastic and inelastic scattered events.
- Multiple scattering correction.
- Calculation of the neutron fluence impinged on the scattering sample, details in Ref. [4, 11].
- Extraction of the differential and the angle integrated cross sections.

The analysis of the waveforms includes the determination of the total integration charge, the correction of the timestamp of the recorded event using the constant fraction discrimination (CFD) algorithm, and the extraction of the pulse shape discrimination (PSD) factor, used for the separation between photon and neutron induced events. Instead of triggering signal analysis at a fixed threshold, the CFD algorithm focuses on a constant fraction of the rising edge of the signal, typically a percentage of its rise time, resulting in an overall improved time resolution [12-14]. The PSD factor was calculated by employing the charge integration method, according to which the factor is determined by the ratio of the integral “tail” of the pulse to the total integral [15-17].

The main background contribution is generated by beam neutrons scattering in the air or surrounding materials and then getting detected by one of the scintillators. To estimate this background, measurements without the sample (sample-out) are performed and then subtracted from the measurement with the sample in place (sample-in). Based on the experiments performed so far at GELINA it is indicated that the background accounts for up to 30-40% of the recorded events per TOF channel. This creates a need for long sample-out measurements in order to have an accurate background subtraction.

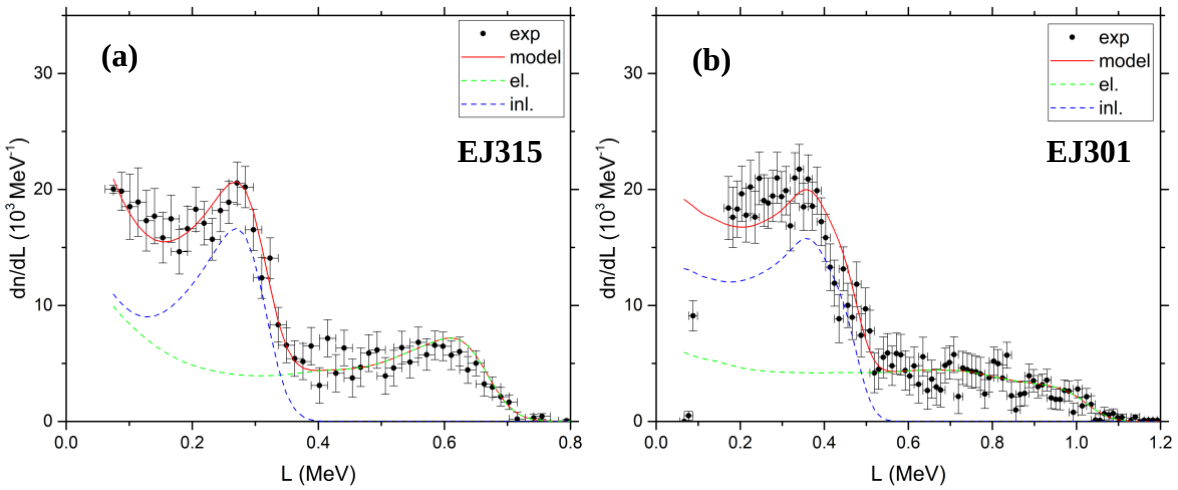

Figure 4. *Light output distributions of the (a) EJ315 and (b) EJ301 detectors at the 142.8º detection angle. The selected 5 ns interval corresponds to E_n = 3.46–3.49 MeV incident neutron energies. The separation between elastic and inelastic scattering from the first excited state of ^{54}Fe is shown [21].*

Once the above steps have been performed, the "clean" neutron time-of-flight spectra have been obtained for each detector. Then, the next step is to identify the scattering reaction process, i.e., separate between events that are coming from elastic or inelastic scattering of a neutron. To do that, the neutron response functions of each scintillator need to be determined. The response function models are calculated for each detector individually by combining experimental data and Monte Carlo simulations. On the one hand, the photon response was determined via measurements with γ-ray sources (^{137}Cs, ^{207}Bi, ^{22}Na, ^{232}Th, AmBe) and simulations using the MCNP6.2 code [18-19]. On the other hand, the neutron response was based on a time-of-flight experiment performed with a carbon sample. In this case, a narrow TOF interval of 5 ns was chosen, in order to obtain light-output distributions for quasi-monoenergetic neutrons. A detailed detector model, utilizing data provided by the manufacturer, was integrated into MCNP6.2. Subsequently, the simulated response to monoenergetic photons and quasi-monoenergetic neutrons were adjusted to match the experimental data. This facilitated the identification of parameters for the detector resolution function and the light output functions [4, 20]. In Fig. 4 an example of the elastic/inelastic separation is presented for a 5 ns time-of-flight interval for detectors.

The multiple scattering correction was performed via Monte Carlo simulations using the MCNP6.2 code. In the simulation, a detailed description of the setup and the neutron beam used in the measurements, based on the fission chamber data analysis, was used. The PTRAC option of MCNP was employed in order to identify neutrons that interacted twice or more with the sample and then arrived at one of the detectors. This method allowed a TOF-dependent and detector-dependent correction to be determined.

The differential scattering cross section was calculated using the following formula:

$$\frac{d\sigma}{d\Omega}(E,\theta) = \frac{N(E,\theta)}{\Delta\Omega \cdot \Phi(E) \cdot \rho_T}$$

where $N(E,\theta)$ is the number of recorded scattered events (elastically or inelastically), $\Delta\Omega$ is the solid angle of the detector, $\Phi(E)$ is the neutron fluence impinged on the scattering sample, and ρ_T is the areal density of the sample. Once the differential cross sections have been calculated for all 8 detection angles, the angle-integrated cross section can be extracted by applying the Gauss-Legendre quadrature rule:

$$\sigma = 2\pi \sum_{i=1}^{8} w_i \cdot \frac{d\sigma}{d\Omega}(cos\theta_i)$$

where $\frac{d\sigma}{d\Omega}(cos\theta_i)$ is the differential cross section as a function of the detection angle, and w_i are the corresponding weighting factors (Table 1).

ACHIEVEMENTS AND FUTURE PLANS

In Table 4 a full list of the experiments performed so far at the ELISA setup is presented. Since the setup became operational, a big focus has been given to the study of neutron elastic scattering on iron. The reason for that is the fact that iron is a major structural material used in a variety of nuclear technology applications, especially in nuclear power reactors, making accurate neutron cross section data indispensable for the design, safe operation, and development of advanced reactor systems. These measurements aim to tackle the lack of hig-resolution experimental data for elastic scattering on iron and assist in sorting out discrepancies between the current nuclear data evaluations.

Table 4. *List of experiments performed so far at the ELISA setup. The nucleus under study, the year of the measurement, the incident neutron energy range under study, and the status of the data analysis are given.*

Nucleus	Year	E_n range (MeV)	Analysis Status
^{nat}Fe	2016	2 – 6	completed
^{nat}C	2016	2 – 6	completed
^{54}Fe	2019	1 – 8	completed
^{nat}C	2020	1 – 8	completed
^{23}Na	2021	1 – 8	in progress
^{56}Fe	2023	1 – 8	in progress

As an example, in Fig. 5, the angle-integrated cross section of neutron elastic scattering on natural iron is presented [5]. The results are compared with the experimental data available in the EXFOR library [22] and the JEFF-3.3 evaluation [23] folded with the experimental energy resolution. There is an overall good agreement between the results of this work with both the evaluation and the rest of the experimental data. It is worth mentioning that this is the first experiment providing high-resolution cross section data for the ^{nat}Fe(n,n) reaction above 2.5 MeV neutron incident energy.

Figure 5. *The angle-integrated cross section of neutron elastic scattering on ^{nat}Fe [5] compared with the available experimental data in the EXFOR library [22] and the JEFF-3.3 evaluation [23] folded with the experimental energy resolution.*

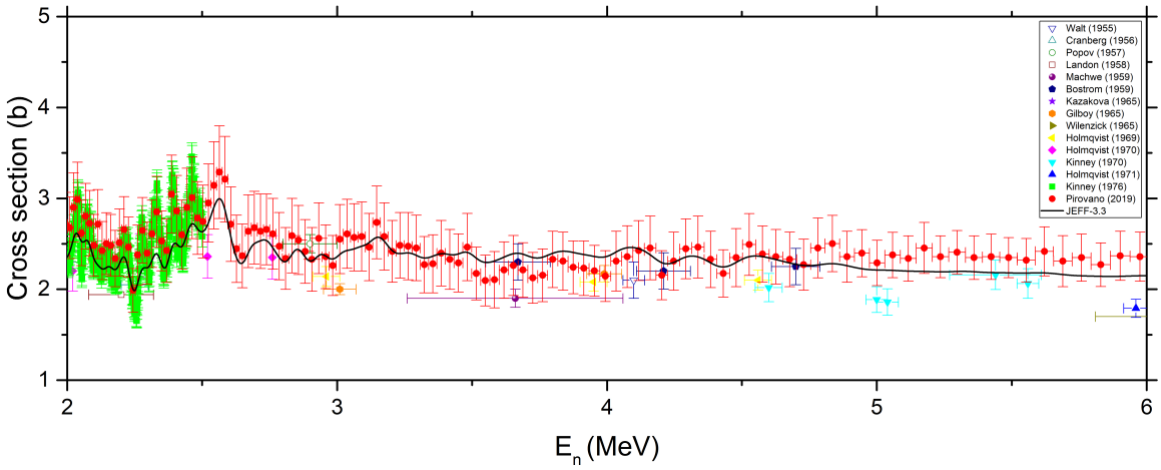

The future plans for the setup are divided into three main axes:

1. Continue the measurements of medium-mass nuclei, where it has been proven that no theoretical model is able to reproduce the fluctuating behavior of the cross section in the 1 - 6 MeV region, meaning that only experimental data can sufficiently constrain the uncertainties on the evaluated

files. The plan for the upcoming years is to continue the work on structural materials by measuring the cross sections of ^{63,65}Cu, but also explore heavy nuclei like ^{206,208}Pb, all cases where there is almost no experimental data for elastic scattering available in the literature.

2. Further development of the spectrometer by installing new detectors. Two options are examined: gamma detectors in order to develop a neutron-gamma coincidence technique that can be used to study nuclei with very low inelastic thresholds, or neutron detectors suitable to measure elastic scattering in neutron incident energies lower than 1 MeV.
3. Reducing the background contribution. As mentioned above, based on the measurements performed so far, the background contribution from the neutron beam scattering in the air accounts for almost 40% of the recorded signals. The plan is to minimize this effect by putting part of the ELISA spectrometer in vacuum conditions. This will be achieved by installing special structures around the setup or in the beam-path.

CONCLUSIONS

This contribution shortly presents the ELISA spectrometer currently installed in the 30m measurements station of the GELINA neutron source at the EC-JRC. The development of the setup, a short description of the analysis procedure, the measurements performed so far, and the future plans for the spectrometer are outlined.

Acknowledgments

The authors would like to thank the technical staff of GELINA for assisting in the development of the spectrometer and providing the conditions needed for the experiments. This work was partially supported by the Commissariat à l'énergie atomique et aux énergies alternatives (CEA) through the SINET project, and by the European Commission through the EUFRAT (EURATOM contract number FP7-211499), and ARIEL (EURATOM research and training program 2014-2018 under grant agreement No 847594) projects.

References

[1] P. Hodgson, Reports on Progress in Physics 47, 613 (1984); doi: 10.1088/0034-4885/47/6/001
[2] R. Varner et al., Physics Reports 201, 57 (1991); doi: 10.1016/0370-1573(91)90039-O
[3] A. Koning et al., Nuclear Physics A 713, 231 (2003); doi: 10.1016/S0375-9474(02)01321-0
[4] E. Pirovano, Ghent University, Ph.D thesis, (2017)
[5] E. Pirovano et al., Physical Review C 99, 024601 (2019); doi: 10.1103/PhysRevC.99.024601
[6] M. Nyman et al., EPJ Web of Conferences 239, 17003 (2020); doi: 10.1051/epjconf/202023917003
[7] E. Pirovano et al., EPJ Web of Conferences 146, 11008 (2017); doi: 10.1051/epjconf/201714611008
[8] W. Mondelaers et al., Notiziario neutroni e luci di sincroton 11, 19-25 (2010)
[9] Eljen Technology, EJ315 data sheet available at: https://eljentechnology.com/products/liquid-scintillators/ej-315 (date accessed: 2024)
[10] Eljen Technology, EJ301, EJ309 data sheet available at: https://eljentechnology.com/products/liquid-scintillatros/ej-301-ej-309 (date accessed: 2024)
[11] C. Rouki et al., NIM A 672, 82 (2012); doi: 10.1016/j.nima.2012.01.004
[12] D.A. Gedcke et al., NIM 55, 377 (1967); doi: 10.1016/0029-554X(67)90145-0
[13] L. Bardelli et al., NIM A 521, 480 (2004); doi: 10.1016/j.nima.2003.10.106
[14] M.A. Nelson et al., NIM A 202, 324 (2003); doi: 10.1016/S0168-9002(03)01078-7
[15] I.A. Pawelczak et al., NIM A 711, 21 (2013); doi: 10.1016/j.nima.2013.01.028
[16] F.D. Brooks, NIM 4, 151 (1959); doi: 10.1016/0029-554X(59)90067-9
[17] J.K. Polack et al., NIM A 795, 253; doi: 10.1016/j.nima.2015.05.048
[18] C.J. Werner et al., Los Alamos National Laboratory, report LA-UR-18-20808 (2018)
[19] C.J. Werner et al., Los Alamos National Laboratory, report LA-UR-17-29981 (2017)
[20] N. Kornilov et al., NIM A 599, 226 (2009); doi: 10.1016/j.nima.2008.10.032
[21] G. Gkatis et al., Phys. Rev. C 109, 034612 (2024); doi: 10.1103/PhysRevC.109.034612
[22] N. Otuka et al., Nuclear Data Sheets 120, 272 (2014); doi: 10.1016/j.nds.2014.07.065
[23] A. Plompen et al., EPJ A 56, (2020); doi: 10.1140/epja/s10050-020-00141-9